

Synthesis, Stabilities, and Redox Behavior of Di(1-azulenyl)(6-azulenyl)methylmethyl Hexafluorophosphates. Generation of a Donor–Acceptor-Substituted Neutral Radical by Azulenes

Shunji Ito,^{*,†} Takahiro Kubo,[†] Noboru Morita,[†] Tadaaki Ikoma,[‡] Shozo Tero-Kubota,[‡] and Akio Tajiri[§]

Department of Chemistry, Graduate School of Science, Tohoku University, Sendai 980-8578, Japan, Institute of Multidisciplinary Research for Advanced Materials, Tohoku University, Sendai 980-8577, Japan, and Department of Materials Science, Faculty of Science and Technology, Hirosaki University, Hirosaki 036-8561, Japan

ito@funorg.chem.tohoku.ac.jp

Received July 22, 2003

Several di(1-azulenyl)(6-azulenyl)methanes and 1,3-bis[(1-azulenyl)(6-azulenyl)methyl]azulenes were prepared by the condensation reaction of azulenes with diethyl 6-formylazulene-1,3-dicarboxylate under acidic conditions. The products were converted into di(1-azulenyl)(6-azulenyl)methylmethyl hexafluorophosphates and azulene-1,3-diylbis[(1-azulenyl)(6-azulenyl)methylmethyl] bis-(hexafluorophosphate)s via hydride abstraction reaction with DDQ following the exchange of counterions. These mono- and dicationic species exhibited high stability with large pK_R^+ values (5.6–10.1), despite the *capto-dative* substitution of azulenes. The electrochemical reduction of the monocations upon cyclic voltammetry (CV) exhibited a reversible two-step, one-electron reduction wave with a small difference between the first reduction potential (E_1^{red}) and the second one (E_2^{red}), which exhibited the generation of highly amphoteric neutral radicals in solution. The electrochemical reduction of dicationic species showed voltammograms, which were characterized by subsequent two single-electron waves and a two-electron transfer upon CV attributable to the formation of a radical cation, a diradical (or twitter ionic structure), and a dianionic species, respectively. Formation of a persistent neutral radical from a monocation was revealed by ESR and UV–vis spectroscopies and theoretical calculations. The ESR spectra of the neutral radical gave two hyperfine coupling constants: $a_H = 0.083$ (6H) and 0.166 mT (9H) ($g = 2.0024$), indicating that an unpaired electron delocalizes over all three of the azulene rings. The stable monoanion, which shows the localization of the charge on the 6-azulenyl substituent, was also successfully generated from the di(1-azulenyl)(6-azulenyl)methane derivative.

Introduction

Recently, much attention has been focused on multi-stage redox systems because of their special properties such as conductivity and organic ferromagnetism.¹ Stabilization of the radical state produced by the redox cycle is fairly important in the construction of materials with potentially useful electronic properties, because the molecules for the application require excellent redox-stability.² Azulene (C₁₀H₈) has attracted the interest of many research groups due to its unusual properties as well as its beautiful blue color.³ Especially, the azulene system has a tendency to stabilize cations, as well as anions, owing to its remarkable polarizability. In addition

to the stabilization of the ionic state, the simultaneous substitution with a donor and an acceptor positions of azulenes might stabilize neutral radicals by the *capto-dative* substitution effect,⁴ although the effect admits of argument.⁵ Donor- and acceptor-substituted neutral radicals, e.g., 2-cyano-10-methyl-5-phenazinyll, have been examined as the conducting materials composed of one

(2) (a) Hünig, S.; Kemmer, M.; Wenner, H.; Perepichka, I. F.; Bäuerle, P.; Emge, A.; Gescheid, G. *Chem. Eur. J.* **1999**, *5*, 1969–1973. (b) Hünig, S.; Kemmer, M.; Wenner, H.; Barbosa, F.; Gescheid, G.; Perepichka, I. F.; Bäuerle, P.; Emge, A.; Peters, K. *Chem. Eur. J.* **2000**, *6*, 2618–2632. (c) Hünig, S.; Perepichka, I. F.; Kemmer, M.; Wenner, H.; Bäuerle, P.; Emge, A. *Tetrahedron* **2000**, *56*, 4203–4211. (d) Hünig, S.; Langels, A.; Schmittel, M.; Wenner, H.; Perepichka, I. F.; Peters, K. *Eur. J. Org. Chem.* **2001**, 1393–1399.

(3) (a) Zeller, K.-P. Azulene. In *Houben-Weyl; Methoden der Organischen Chemie*, 4th ed.; Georg Thieme: Stuttgart, Germany, 1985; Vol. V, Part 2c, pp 127–418. (b) Lemaal, D. M.; Goldman, G. D. *J. Chem. Edu.* **1988**, *65*, 923–925.

(4) (a) Stella, L.; Janousek, Z.; Merényi, R.; Viehe, H. G. *Angew. Chem., Int. Ed. Engl.* **1978**, *17*, 691–692. (b) Viehe, H. G.; Merényi, R.; Stella, L.; Janousek, Z. *Angew. Chem., Int. Ed. Engl.* **1979**, *18*, 917–932. (c) Viehe, H. G.; Janousek, Z.; Merényi, R. *Acc. Chem. Res.* **1985**, *18*, 148–154.

* Address correspondence to this author. Phone: +81-22-217-7714. Fax: +81-22-217-7714.

[†] Graduate School of Science, Tohoku University.

[‡] Institute of Multidisciplinary Research for Advanced Materials, Tohoku University.

[§] Hirosaki University.

(1) Deuchert, K.; Hünig, S. *Angew. Chem., Int. Ed. Engl.* **1978**, *17*, 875–886.

CHART 1

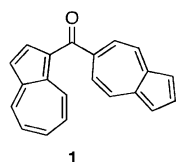
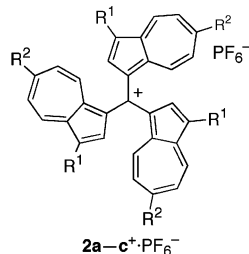


CHART 2



a: R¹ = R² = H, **b:** R¹ = R² = *t*-Bu, **c:** R¹ = H, R² = OMe

kind of molecule.⁶ Phenalenyl radicals having donor and acceptor substituents have been produced as highly amphoteric hydrocarbons.⁷ Preparation of the azulene derivatives incorporating the *capto-dative* substituent effect would also provide an opportunity to construct a reversible redox system with high redox-stability. In addition to the redox-stability, the azulene derivatives should exhibit strong absorption in the visible region in both cationic and anionic states.^{8–10} The molecules might be applied to the preparation of novel polyelectrochromic materials with high redox-stability.¹¹ However, no attempt has made to generate such a stabilized neutral radical utilizing *capto-dative* substitution of azulenes, to our knowledge, although the redox properties of 1,6'-diazulenyl ketone (**1**) have been examined for a potential precursor for such a system (Chart 1).¹²

We have recently reported the synthesis of tri(1-azulenyl)methyl cation hexafluorophosphates (e.g., **2a–c**⁺·PF₆[−]) with high thermodynamic stabilities (Chart 2).¹³ In view of the extreme stabilities of the tri(1-azulenyl)-

(5) (a) Birkhofer, H.; Hädrich, J.; Beckhous, H.-D.; Rüchardt, C. *Angew. Chem., Int. Ed. Engl.* **1987**, *26*, 573–575. (b) Beckhous, H.-D.; Rüchardt, C. *Angew. Chem., Int. Ed. Engl.* **1987**, *26*, 770–771.

(6) Nakasuji, K.; Yamaguchi, M.; Murata, I.; Yamaguchi, K.; Fueno, T.; Ohya-Nishiguchi, H.; Sugano, T.; Kinoshita, M. *J. Am. Chem. Soc.* **1989**, *111*, 9265–9267.

(7) Awaga, K.; Sugano, T.; Kinoshita, M. *Bull. Chem. Soc. Jpn.* **1985**, *58*, 1886–1893.

(8) Ito, S.; Inabe, H.; Morita, N.; Ohta, K.; Kitamura, T.; Imafuku, K. *J. Am. Chem. Soc.* **2003**, *125*, 1669–1680.

(9) (a) Ito, S.; Inabe, H.; Okujima, T.; Morita, N.; Watanabe, M.; Harada, N.; Imafuku, K. *J. Org. Chem.* **2001**, *66*, 7090–7101. (b) Ito, S.; Okujima, T.; Morita, N. *J. Chem. Soc., Perkin Trans. 1* **2002**, 1896–1905.

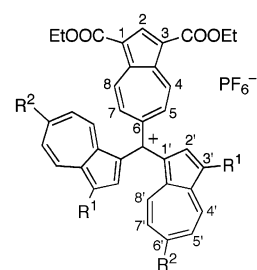
(10) Ito, S.; Nomura, A.; Morita, N.; Kabuto, C.; Kobayashi, H.; Maejima, S.; Fujimori, K.; Yasunami, M. *J. Org. Chem.* **2002**, *67*, 7295–7302.

(11) (a) Monk, P. M. S.; Mortimer, R. J.; Rosseinsky, D. R. *Electrochromism: Fundamentals and Applications*; VCH: Weinheim, Germany, 1995. (b) Komatsu, T.; Ohta, K.; Fujimoto, T.; Yamamoto, I. *J. Mater. Chem.* **1994**, *4*, 533–536. (c) Rosseinsky, D. R.; Monk, D. M. S. *J. Appl. Electrochem.* **1994**, *24*, 1213–1221.

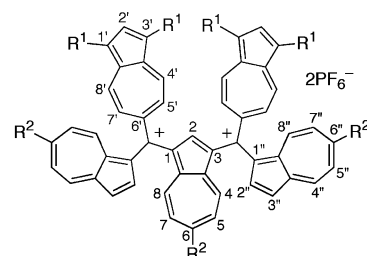
(12) Kurotobi, K.; Takakura, K.; Murafuji, T.; Sugihara, Y. *Synthesis* **2001**, 1346–1350.

(13) (a) Ito, S.; Morita, N.; Asao, T. *Bull. Chem. Soc. Jpn.* **1995**, *68*, 1409–1437. (b) Ito, S.; Kikuchi, S.; Morita, N.; Asao, T. *Bull. Chem. Soc. Jpn.* **1999**, *72*, 839–849. (c) Ito, S.; Kikuchi, S.; Morita, N.; Asao, T. *J. Org. Chem.* **1999**, *64*, 5815–5821. (d) Ito, S.; Morita, N.; Asao, T. *Bull. Chem. Soc. Jpn.* **2000**, *73*, 1865–1874. (e) Ito, S.; Kikuchi, S.; Okujima, T.; Morita, N.; Asao, T. *J. Org. Chem.* **2001**, *66*, 2470–2479.

CHART 3

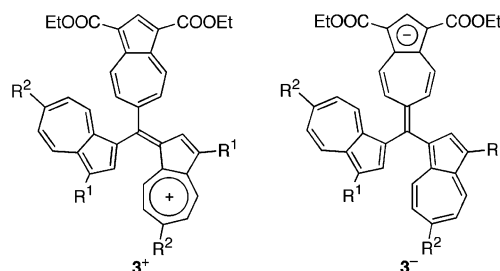


3a⁺·PF₆[−]: R¹ = R² = H
3b⁺·PF₆[−]: R¹ = R² = *t*-Bu
3c⁺·PF₆[−]: R¹ = H, R² = OMe

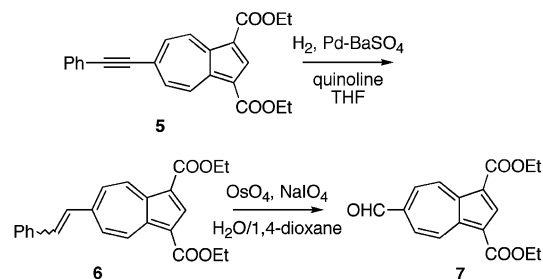


4a²⁺·2PF₆[−]: R¹ = COOEt, R² = H
4b²⁺·2PF₆[−]: R¹ = COOEt, R² = OMe

CHART 4

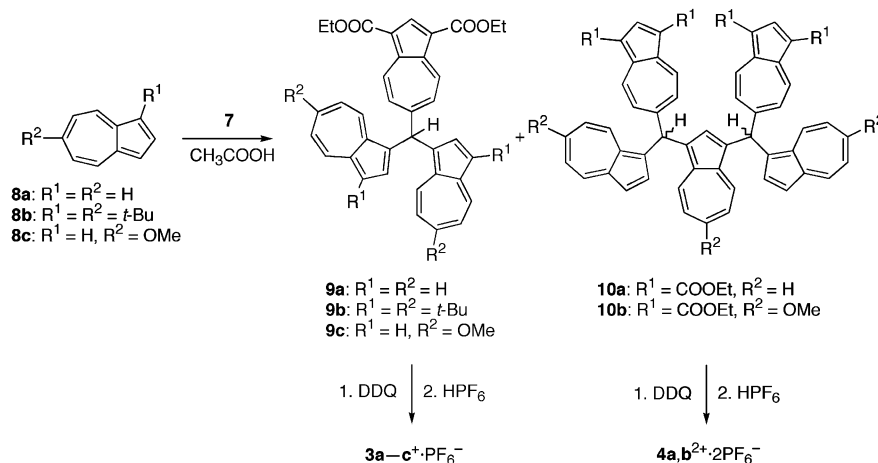


SCHEME 1



methyl cations, we have now prepared stable methyl cations incorporating a 6-azulenyl substituent, i.e., di(1-azulenyl)(6-azulenyl)methyl cation hexafluorophosphates **3a–c**⁺·PF₆[−] and azulene-1,3-diylyl[(1-azulenyl)(6-azulenyl)methyl cation] bis(hexafluorophosphate)s **4a,b**²⁺·2PF₆[−] (Chart 3), which should exhibit high stabilities in both cationic and anionic states by the contribution of the tropylium and cyclopentadienide substructures (**3**⁺ and **3**[−]) in addition to the neutral radical by the *capto-dative* substituent effect (Chart 4). The formation of a persistent neutral radical from monocation **3b**⁺ was revealed by ESR and UV–vis spectroscopies and theoretical calculations. The present report also describes the generation of stable monoanion **3b**[−] by the deprotonation of the corresponding methane derivative.

SCHEME 2



Results and Discussion

Preparation of the carbaldehyde **7**¹⁴ commenced with 6-phenylethynylazulene **5**^{9a,15} and is outlined in Scheme 1. Partial hydrogenation of the alkyne **5** utilizing Pd–BaSO₄ as a catalyst in the presence of quinoline gave an olefin **6**¹⁶ as a single stereoisomer. However, unequivocal analysis of the stereochemistry of **6** was hampered by the chemical shift equivalents of both olefin protons on the ¹H NMR spectrum. The olefin **6** was converted into **7** by oxidative cleavage utilizing OsO₄–NaIO₄ in 82% yield from **5**.¹⁷

The reaction of two molar amounts of azulene (**8a**) and its 1,6-di-*tert*-butyl (**8b**) and 6-methoxy (**8c**) derivatives with **7** in acetic acid at room temperature afforded **9a–c** in 23–80% yields, along with diastereomeric mixtures of 1,3-bis{(1-azulenyl)[1,3-bis(ethoxycarbonyl)-6-azulenyl]-methyl}azulenes **10a** (19%) and **10b** (10%) in the case of **8a** and **8c** (Scheme 2). The high-pressure reaction (10 kbar)¹⁸ of **8c** with **7** in a 50% acetic acid solution of dichloromethane at 40 °C for 1 day slightly increased the yields of the desired **9c** (26%) and **10b** (18%).

Synthesis of the monocations **3a–c⁺** and the dication **4a,b²⁺** was accomplished by the hydride abstraction from **9a–c** and **10a,b**, respectively. The reaction of **9a–c** with DDQ in dichloromethane at room temperature, followed by an addition of a 60% aqueous HPF₆ solution, yielded **3a–c⁺** (70–88%) as a hexafluorophosphate (Scheme 2).¹³ Similarly, the oxidation of **10a** and **10b** with 2 molar equiv of DDQ, followed by the addition of an HPF₆ solution, afforded the corresponding bis(hexafluorophosphate)s **4a,b²⁺·2PF₆⁻** in 78% and 75% yields, respectively (Scheme 2). These new salts **3a–c⁺·PF₆⁻** and **4a,b²⁺·2PF₆⁻** are stable, deep-colored crystals, and are storable in the crystalline state.

Mass spectra of **3a–c⁺·PF₆⁻** and **4a,b²⁺·2PF₆⁻** ionized by FAB showed the correct M⁺ – PF₆ ion peaks, together

TABLE 1. The Longest Wavelength Absorptions and Coefficients of **3a–c⁺·PF₆⁻**, **4a,b²⁺·2PF₆⁻**, and **2a–c⁺·PF₆⁻** in Acetonitrile

sample	λ _{max} , nm (log ε)	sample	λ _{max} , nm (log ε)
3a⁺·PF₆⁻	675 (4.42)	4b²⁺·2PF₆⁻	712 (4.45), 603 (4.21)
3b⁺·PF₆⁻	719 (4.59)	2a⁺·PF₆⁻	614 (4.70)
3c⁺·PF₆⁻	668 (4.53)	2b⁺·PF₆⁻	650 (4.62)
4a²⁺·2PF₆⁻	718 (4.51), 608 (4.27)	2c⁺·PF₆⁻	620 (4.87)

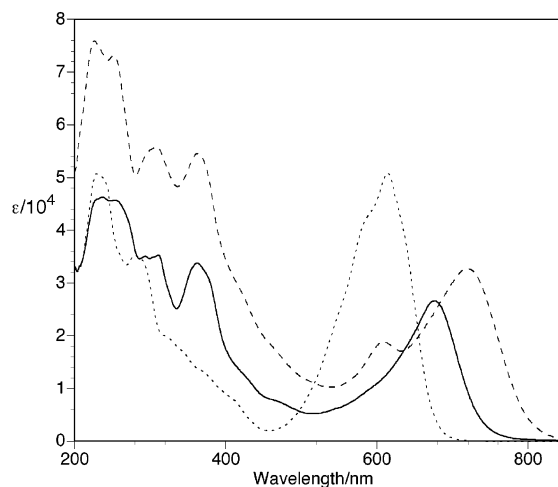


FIGURE 1. UV–vis spectra of **3a⁺** (solid line), **4a²⁺** (broken line), and **2a⁺** (dotted line) in acetonitrile.

with M⁺ – 2PF₆ ion peaks in the case of **4a,b²⁺·2PF₆⁻**. The characteristic bands of hexafluorophosphate were observed at 841–843 (strong) and 558 (medium) cm⁻¹ in their IR spectra. These salts showed strong absorption in the visible region, as did the salts **2a–c⁺·PF₆⁻**, and so on.¹³ Their absorption maxima (nm) and coefficients (log ε) are summarized in Table 1. UV–vis spectra of **3a⁺** and **4a²⁺** in acetonitrile along with that of **2a⁺** are shown in Figure 1. The longest wavelength absorption of **3a–c⁺** showed an appreciable bathochromic shift by 61, 69, and 48 nm, respectively, compared with those of **2a–c⁺**. The UV–vis spectra of **4a,b²⁺** in the visible region were characterized by two strong absorption bands as summarized in Table 1, although **3a–c⁺** exhibited an absorp-

(14) Morita, T.; Fujita, T.; Nakadate, T.; Takase, K. *Sci. Rep. Tohoku Uni., Ser. I* **1980**, *62*, 91–101.

(15) Morita, T.; Fujita, T.; Takase, K. *Bull. Chem. Soc. Jpn.* **1980**, *53*, 1647–1651.

(16) Matsumura, H.; Nagamura, S. *Nippon Kagaku Zasshi* **1964**, *85*, 901–905.

(17) (a) Saito, M.; Morita, T.; Takase, K. *Bull. Chem. Soc. Jpn.* **1980**, *53*, 3696–3700. (b) Balschukat D.; Dehmow, E. V. *Chem. Ber.* **1986**, *119*, 2272–2288.

(18) Matsumoto, K.; Sera, A.; Uchida, T. *Synthesis* **1985**, 1–26.

TABLE 2. pK_R^+ Values^a and Redox Potentials^b of $3a-c^+$, $4a,b^{2+}$, and $2a-c^+$

cation	pK_R^+	E_1^{red}	E_2^{red}	E_3^{red}	E_1^{ox}	E_2^{ox}	E_3^{ox}
3a⁺	8.1 ± 0.2 (26%) ^c	-0.46	-0.69	(-1.99)	(+1.00)	(+1.33)	
3b⁺	10.1 ± 0.2 (19%) ^c	-0.56	-0.73		+0.89	(+1.29)	(+1.39)
3c⁺	9.5 ± 0.3 (68%) ^c	-0.53	-0.71		(+0.92)	(+1.35)	
4a²⁺	5.6 ± 0.1, 8.1 ± 0.1	-0.26	(-0.41)	(-0.76)	(+1.18)	(+1.27)	
		-0.22 ^d	-0.39 ^d	-0.76 ^d	+1.14 ^d	+1.19 ^d	
4b²⁺	8.5 ± 0.2	-0.34	-0.52	-0.74	(+1.05)	(+1.24)	
		-0.30 ^d	-0.48 ^d	-0.71 ^d	+1.02 ^d	+1.23 ^d	
2a⁺	11.3	-0.78	(-1.56)		(+0.98)	(+1.07)	
2b⁺	14.3	-0.91	(-1.72)		+0.84	+0.95	(+1.50)
2c⁺	>14.0	-0.88	(-1.64)		(+0.90)	(+0.98)	

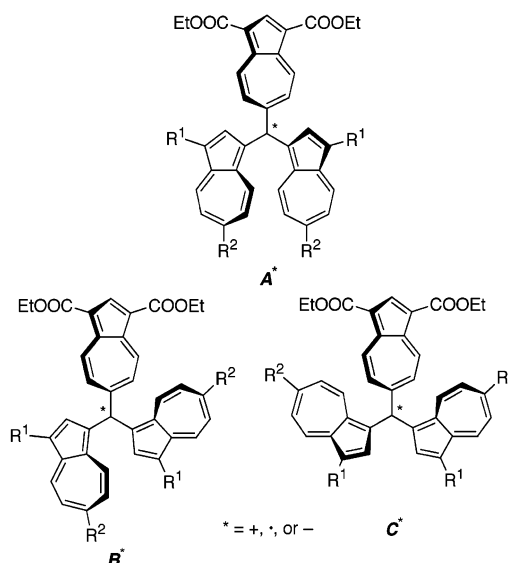
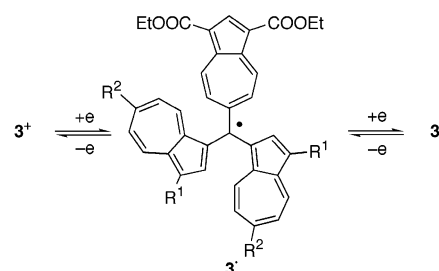
^a pK_R^+ values were determined spectrophotometrically at 25 °C in a buffered solution prepared in 50% aqueous acetonitrile. ^b Redox potentials were measured by CV (0.1 M Et₄NClO₄ in acetonitrile, Pt electrode, scan rate 100 mV s⁻¹, and ferrocene/ferrocenium = 0.07 V). In the case of irreversible waves, which are given in parentheses, E_{ox} and E_{red} were calculated as E_{pa} (anodic peak potential) - 0.03 and E_{pc} (cathodic peak potential) + 0.03 V, respectively. ^c Regenerated absorption maxima (%) of the cations in the visible region by the immediate acidification of the alkaline solution with HCl after the pK_R^+ measurement are given in parentheses. ^d Redox potentials measured by DPV.

tion band in this region. The longest wavelength absorption of **4a,b²⁺** showed an appreciable bathochromic shift by 43 and 44 nm, respectively, compared with those of **3a⁺** and **3c⁺**, similar to the results on the dications stabilized by 1-azulenyl groups.^{13d,e} The bathochromic shift of **4a,b²⁺** should be attributable to the increase of the positive charge at the central cationic carbons, because the two cation units of the dications **4a,b²⁺** were stabilized by three 1-azulenyl groups in contrast to the stabilization by two 1-azulenyl groups in the case of the monocations **3a-c⁺**.

The ¹H NMR chemical shifts of the methine protons of **9a-c** (**9a**, 7.03 ppm; **9b**, 6.93 ppm; and **9c**, 6.89 ppm) showed a slight upfield shift, compared with those of tri(1-azulenyl)methane (7.36 ppm) and its 1,1',1'',6,6',6''-hexa-*tert*-butyl (7.08 ppm) and 6,6',6''-trimethoxy (7.15 ppm) derivatives.^{13a,b} Those of **10a** and **10b** were also observed at a slight upfield location (**10a**, 6.96 and 6.93 ppm; and **10b**, 7.07 ppm) compared with those of tri(1-azulenyl)methane and its 6,6',6''-trimethoxy derivative. These signals disappeared on the ¹H NMR spectra of **3a-c⁺** and **4a,b²⁺**. Thus, the ¹H NMR spectra also supported the cationic structure of these compounds.

It is possible for **3a-c⁺** to exhibit the three isomeric propeller conformations excluding enantiomeric forms (**A⁺**, **B⁺**, and **C⁺**) as illustrated in Figure 2.^{13a} Despite the presumed stereoisomerism, the ¹H and ¹³C NMR spectra of **3a-c⁺** were observed as the time-averaged spectra of these three conformers at room temperature. In the case of **4a,b²⁺** we could not obtain well-resolved ¹H NMR spectra, probably due to the presumed stereoisomerism. The spectra are represented in the Supporting Information.

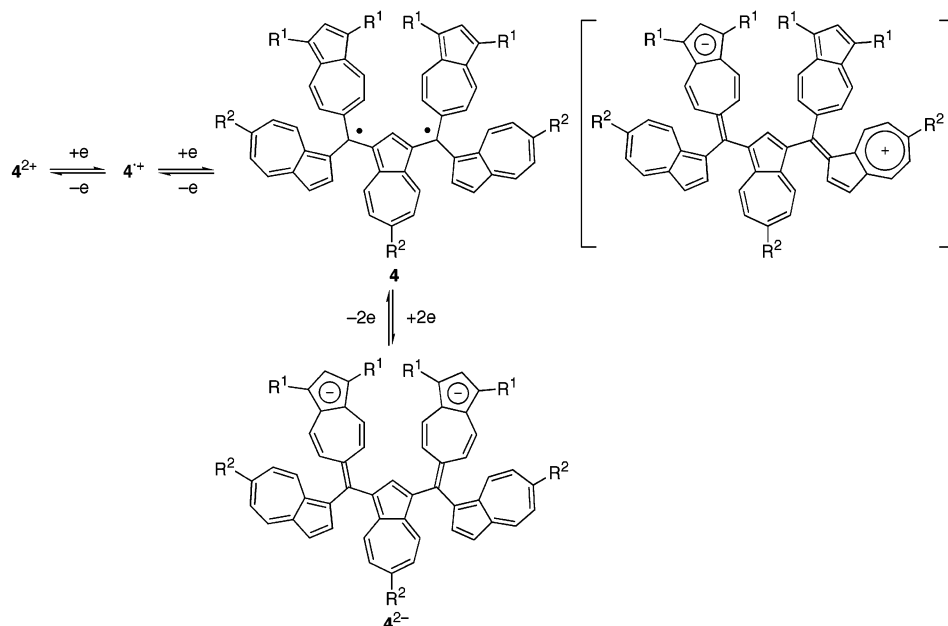
Large downfield shifts were observed at H-4', 5', 6', and 7' protons on **3a-c⁺** as compared with those of the methane derivatives **9a-c**. The largest $\Delta\delta$ value was observed at H-5', i.e., +0.97 ppm for **3a⁺**, +0.98 ppm for **3b⁺**, and +0.86 ppm for **3c⁺**. The large downfield shifts in the seven-membered ring protons of 1-azulenyl substituents are consistent with the azulenylium ion substructure of **3a-c⁺**. The upfield shifts of H-8' in **3a-c⁺** should be regarded as being the effect of the neighboring azulenyl substituents. The chemical shifts (¹³C NMR) of the central cationic carbons in **3a-c⁺**·PF₆⁻ (**3a⁺**, 164.5 ppm; **3b⁺**, 159.9 ppm; and **3c⁺**, 163.2 ppm) were observed at slightly downfield location compared with those in **2a-**

**FIGURE 2.** Presumed conformational isomers for **3⁺**.**SCHEME 3**

c⁺ (**2a⁺**, 157.4 ppm; **2b⁺**, 151.8 ppm; and **2c⁺**, 156.3 ppm).^{13a,b} In analogy with the results on ¹H NMR measurements, large $\Delta\delta$ values were observed at 3', 3'a-, 5', 7', and 8'a-carbons. Therefore, the NMR spectra of **3a-c⁺** revealed that most of the positive charge is delocalized on 1-azulenyl substituents as an azulenylium ion substructure, which contributes to the stability of the carbocations.

As a measure of the thermodynamic stability of the carbocations, the pK_R^+ values of monocations **3a-c⁺** and dications **4b,c²⁺** were determined spectrophotometrically at 25 °C in a buffer solution prepared in 50% aqueous

SCHEME 4



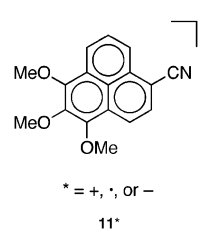
acetonitrile.^{13,19} The pK_R^+ scale stands for the carbocation in aqueous solution ($pK_R^+ = -\log K_R^+$). The K_R^+ scale is defined by the equilibrium constant for the reaction of a carbocation with a water molecule ($K_R^+ = [ROH][H_3O^+]/[R^+]$). Therefore, the larger pK_R^+ index indicates higher stability of the carbocation. The values of **3a-c**⁺ and **4a,b**²⁺ are summarized in Table 2 along with those of the corresponding tri(1-azulenyl)methyl cations **2a-c**⁺.

The pK_R^+ values of **3a-c**⁺ exhibited destabilization compared with those of **2a-c**⁺ due to the substitution of the electron-withdrawing 6-azulenyl group. However, **3a-c**⁺ still exhibit large pK_R^+ values (8.1–10.1), which provide a criterion of high thermodynamic stability of these cations. These values are 14.5–16.5 pK units higher than that of the triphenylmethyl cation ($pK_R^+ = -6.4$).²⁰ The *tert*-butyl substituents on each azulene ring slightly increased the pK_R^+ value due to their steric effect, and also by their inductive electronic effect induced by the C–C hyperconjugation with the systems.

Two cation units in **4a**²⁺ were neutralized stepwise at the pH of 5.6 and 8.1, respectively. Thus, the dication **4a**²⁺ itself is even more destabilized than the monocation **3a**⁺ by 2.5 pK units. However, the half-neutralized monocation of **4a**²⁺ was as stable as the monocation **3a**⁺. In the case of **4b**²⁺, two cation units were neutralized simultaneously at the pH of 8.5. The pH corresponds to the average of the pK_R^{2+} value for the dication and of the pK_R^+ value for the half-neutralized monocation.

The neutralization of these cations is not completely reversible due to the instability of the neutralized products under the conditions of the pK_R^+ measurement. After the measurement, acidification of the alkaline solutions of **3a-c**⁺ with HCl regenerated the characteristic absorption of the carbocations in the visible region

CHART 5



in 19–68% (Table 2). The instability of the neutralized products should be attributed to the production of an unstable polyolefinic substructure by the attack of the base to the aromatic core. Indeed, the base treatment of **3b**⁺ afforded a significantly complex mixture, which did not reproduce the corresponding cation **3b**⁺ anymore.

To clarify the electrochemical property, the redox behavior of **3a-c**⁺ and **4a,b**²⁺ was examined by cyclic voltammetry (CV) and differential pulse voltammetry (DPV) and compared with those of **2a-c**⁺. Redox potentials (in volts vs Ag/Ag⁺) of **3a-c**⁺ and **4a,b**²⁺ are summarized in Table 2, together with those of **2a-c**⁺. The reduction waves of **3b**⁺ and **4b**²⁺ are shown in the Supporting Information. The cyclic voltammogram of **3a-c**⁺ exhibited two reversible redox waves ($E_{1/2} = -0.46$ to -0.56 V and -0.69 to -0.73 V upon CV) that should correspond to two single-electron transfers (Scheme 3). The formation of neutral radical **3•** and anion **3⁻** was revealed by the ESR observation of **3b•**, generation of **3b⁻** by the reaction of **9b** with potassium *tert*-butoxide, and also electrochromic analysis of monocation **3b**⁺. The less negative reduction potential of these cations, compared with that of **2a-c**⁺, corresponds to the increase of electron affinity of the cations by the 6-azulenyl substituent. The potential difference between the first and the second reduction waves (0.17–0.23 V) is significantly small as compared with those of **2a-c**⁺ (0.76–0.81 V). These results indicated the generation of neutral radicals **3a-c•** with substantial amphoteric redox property. The amphoteric redox nature of **3a-c•** is significantly higher

(19) (a) Kerber, R. C.; Hsu, H. M. *J. Am. Chem. Soc.* **1973**, *95*, 3239–3245. (b) Komatsu, K.; Masumoto, K.; Waki, Y.; Okamoto, K. *Bull. Chem. Soc. Jpn.* **1982**, *55*, 2470–2479.

(20) Arnett E. M.; Buhick, R. D. *J. Am. Chem. Soc.* **1964**, *86*, 1564–1571.

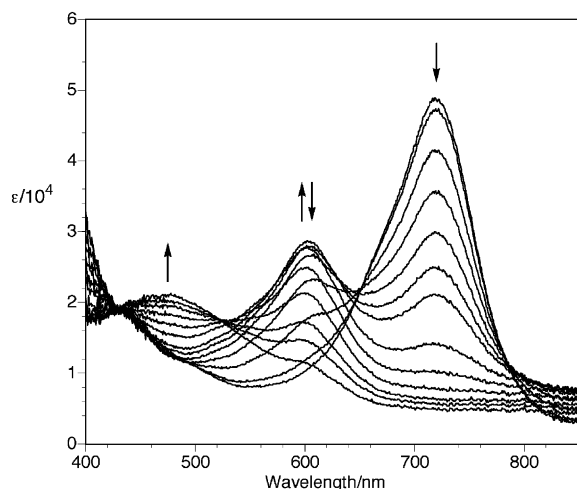


FIGURE 3. Continuous change in visible spectra of $3b^+$ (2 mL; 0.2×10^{-5} M) in acetonitrile containing Et_4NClO_4 (0.1 M) upon constant-current electrochemical reduction (100 μ A) at 10- (lines 1–7) or 20-s (lines 8–13) intervals.

than that of donor- and acceptor-substituted phenalenyl radical 11^\bullet (Chart 5), which showed high redox stability ($E_1^{\text{red}} - E_2^{\text{red}}$ of phenalenyl cation 11^+ is reported as 1.09 V).⁷ The substantial amphoteric redox property of $3a-c^\bullet$ could be explained by the *capto-dative* substitution effect of the azulenyl groups.

The electrochemical reduction of $4a,b^{2+}$ showed a barely separated, three-step reduction wave, which was characterized by subsequent two single-electron waves and a two-electron transfer at $E_{1/2} = -0.26$ to -0.83 V upon CV. The first two single-electron waves suggest the redox interaction between the two-cation units. These waves should correspond to the formation of radical cation 4^+ , diradical (or twitter ionic structure) 4 , and dianionic species 4^{2-} , respectively (Scheme 4).

The electrochemical oxidation of $3b^+$ showed a reversible wave at +0.89 V and an irreversible wave at +1.29 V, due to the oxidation of azulene rings, to give a dication radical and a tricationic species. The electrochemical oxidation of cations $3a^+$ and $3c^+$ exhibited irreversible waves at +1.00 and +0.92 V, respectively. The oxidation behavior of $3a-c^+$ is almost comparable to that of di(1-azulenyl)phenylmethyl cations.^{13a} The electrochemical oxidation of $4a,b^{2+}$ also exhibited irreversible waves at +1.05 to +1.27 V upon CV.

When the UV–vis spectra of $3b^+$ were measured under the electrochemical reduction conditions, a new absorption (602 nm) in the visible region was gradually developed as shown in Figure 3. The color of the solution gradually changed from deep-green to deep-blue during electrochemical reduction. On further reduction the new band in the visible region gradually decreased accompanied by the change of the deep-blue color to deep-red. The reverse oxidation of the red-colored solution regenerated the UV–vis spectra of the deep-green $3b^+$. Thus, the color change of the solution should correspond to the formation of anion $3b^-$ via neutral radical $3b^\bullet$ in two-electron reduction, as observed upon CV.

Formation of $3b^\bullet$ from $3b^+$ was confirmed by the ESR measurements, which were carried out at room temperature with use of a degassed acetonitrile solution pre-

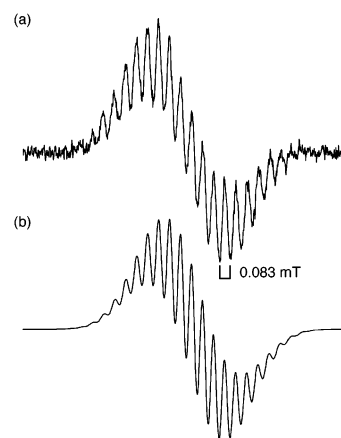


FIGURE 4. ESR spectrum of $3a^\bullet$ generated by the electrochemical reduction in acetonitrile at room temperature: (a) observed ESR spectrum and (b) computer simulation.

pared under a vacuum line. The deep-green solution of $3b^+$ did not indicate any ESR signal, but the multiline ESR spectrum in Figure 4 appeared with the color change to deep-blue during the electrochemical reduction. This fact indicates that the blue color originates from the radical species of $3b^\bullet$. The ESR spectrum is apparently split into 19 lines due to hyperfine interactions. The simulation with a g -value of 2.0024 and proton hyperfine coupling (hfc) constants of 0.166 (9H) and 0.083 mT (6H) well reproduced the observed spectrum.

We have performed a semiempirical UHF (Unrestricted Hartree–Fock) molecular orbital calculation using an AM1 (Austin Model 1) Hamiltonian to estimate the spin density distribution of 3^\bullet without any substituents.²¹ The geometry optimizations starting from several different conformations clarified the presence of three stereoisomers having a local minimum of potential surface. Consideration of the stabilities of the stereoisomers based on the calculated heats of formation demonstrates that conformer **C** (Figure 2) is the most stable stereoisomer, although the difference among them is small (Supporting Information). The spin density distributions calculated for the conformers **A–C** are very similar to each other, which are characterized by the high spin density at 2-, 3a-, 5-, 7-, and 8a-carbons and low density at 1-, 3-, 4-, 6-, and 8-carbons on each azulene ring regardless of the substituted positions. Therefore, the observed ESR spectrum is reasonably explained by the hyperfine interactions from three 2-, 5-, 7-protons and two 4-, 8-protons on each azulene ring to exhibit nine large and six small hfc constants, respectively. Thus, the ESR studies for the neutral radical exhibit that the unpaired electron delocalizes over the three azulene rings.

(21) The molecular orbital calculations were done with a Gaussian revision E.2 program package,²² which was installed in an UNIX workstation under a molecular design support system in IMRAM.

(22) Frisch, M. J.; Trucks, G. W.; Schlegel, H. B.; Gill, P. M. W.; Johnson, B. G.; Robb, M. A.; Cheeseman, J. R.; Keith, T.; Petersson, G. A.; Montgomery, J. A.; Raghavachari, K.; Al-Laham, M. A.; Zakrzewski, V. G.; Ortiz, J. V.; Foresman, J. B.; Cioslowski, J.; Stefanov, B. B.; Nanayakkara, A.; Challacombe, M.; Peng, C. Y.; Ayala, P. Y.; Chen, W.; Wong, M. W.; Andres, J. L.; Replogle, E. S.; Gomperts, R.; Martin, R. L.; Fox, D. J.; Binkley, J. S.; Defrees, D. J.; Baker, J.; Stewart, J. P.; Head-Gordon, M.; Gonzalez, C.; Pople, J. A. Gaussian, revision E.2; Gaussian, Inc.: Pittsburgh, PA, 1995.

SCHEME 5

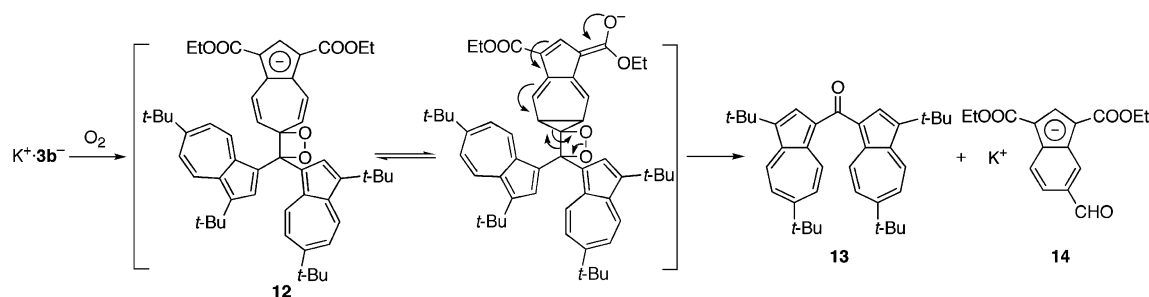
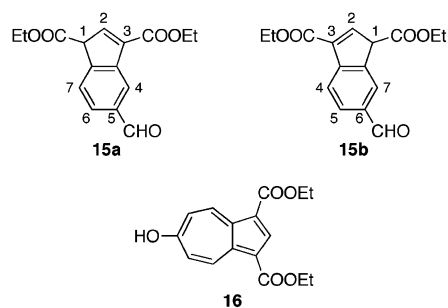


CHART 6



The neutral radical was considerably stable probably due to the protection by the 3'- and 6'-*tert*-butyl groups and 1,3-diethoxycarbonyl substituents in addition to the highly delocalized structure by the *capto-dative* substitution. Indeed, the deep blue color of the neutral radical **3b[•]** was persistent even under aerobic conditions at room temperature ($T_{1/2} = 39$ min). The radical persisted for a much longer period under degassed conditions ($T_{1/2} = 4.4$ days).

The anion **3b⁻** was generated as a red solution by the reaction of **9b** with potassium *tert*-butoxide in a tetrahydrofuran solution. The anion **3b⁻** was found to be stable at room temperature in a degassed solution. The UV-vis spectrum of **3b⁻** in tetrahydrofuran is shown in the Supporting Information. The time-averaged ¹H and ¹³C NMR spectra of **3b⁻**, on which the isomeric propeller conformations expected in the same way of the cation **3b⁺** (Figure 2) can be averaged out, were obtained at room temperature in tetrahydrofuran-*d*₈. The NMR spectra exhibited large chemical shift differences for the positions in the 6-azulenyl substituent as compared with those of the methane derivative **9b**, which correspond to most of the negative charge residing on the 6-azulenyl substituent.

The relatively low stability of the anion **3b⁻** under aerobic conditions is attributable to the high reactivity of **3b⁻** with oxygen to produce bis(3,6-di-*tert*-butyl-1-azulenyl)ketone (**13**) and potassium 1,3-ethoxycarbonyl-5-formylindene-1,3-dicarboxylate (**15a** and **15b**) by the treatment with acid (Chart 6). 6-Hydroxyazulene **16** did not show the rearrangement into the indenide **14** by the reaction with potassium *tert*-butoxide in tetrahydrofuran-*d*₈. Thus, a possible mechanism for the reaction of **3b⁻** with oxygen molecule could be illustrated as shown in Scheme 5.

Conclusion

Several di(1-azulenyl)(6-azulenyl)methyl cations **3a⁻c⁺** and azulene-1,3-diylbis[(1-azulenyl)(6-azulenyl)methyl] dication (**4a,b²⁺**) were prepared by the hydride abstraction reaction of the corresponding methane derivatives. These mono- and dication (**3a⁻c⁺** and **4a,b²⁺**) exhibited high stability with large pK_R^+ values. The monocations **3a⁻c⁺** were found to behave as a two-stage reduction property with a small numerical sum of the first reduction potentials (E_1^{red}) and the second one (E_2^{red}), which exhibited the generation of a highly amphoteric neutral radical in solution. It is noteworthy that the color depending on the charge of **3b[•]** exhibits three primary colors, deep-green for monocation **3b⁺**, deep-blue for neutral radical **3b[•]**, and red for anion **3b⁻**. The dication **4a,b²⁺** showed voltammograms, which were characterized by subsequent two single-electron waves and a two-electron transfer upon CV attributable to the formation of a radical cation, a diradical (or twitter ionic structure), and a dianionic species, respectively.

Experimental Section

General. For general experimental details and instrumentation, see our earlier publication.^{9b}

Diethyl 6-Formylazulene-1,3-dicarboxylate (7). A mixture of **5** (3.72 g, 10.0 mmol), 5 wt % Pd–BaSO₄ (501 mg), and quinoline (511 mg, 3.96 mmol) in THF (150 mL) and water was stirred at room temperature for 6 h under an H₂ atmosphere. After the Pd catalyst was removed by filtration, the solvent was removed under reduced pressure. Purification of the residue by column chromatography on silica gel with CH₂Cl₂ afforded **6**. To a solution of **6** in 1,4-dioxane (115 mL) and water (45 mL) was added 2 wt % osmium(VIII) oxide in 1,4-dioxane (30.2 g, 2.38 mmol). Then, sodium periodate (6.68 g, 31.2 mmol) was added over a period of 30 min. After the mixture was stirred at room temperature for 5.5 d, it was poured into water and extracted with CH₂Cl₂. The organic layer was washed with water, dried with MgSO₄, and concentrated under reduced pressure. The residue was purified by column chromatography on silica gel with CH₂Cl₂ to afford **7** (2.42 g, 82%) as deep green powder. Mp 181.1–182.2 °C (hexane); [lit.¹² mp 190–191 °C]; MS (70 eV) *m/z* (rel intensity) 300 (M⁺, 100%), 255 (M⁺ – OEt, 61), 227 (M⁺ – COOEt, 41); IR (KBr disk) ν_{max} 1713 (s, CHO), 1686 (s, C=O) cm⁻¹; UV-vis (CH₂Cl₂) λ_{max} , nm (log ϵ) 247 (4.53), 271 sh (4.18), 305 sh (4.66), 317 (4.78), 342 sh (3.84), 352 (3.93), 362 sh (3.85), 379 (3.72), 535 sh (2.57), 579 (2.70), 625 sh (2.61), 690 sh (2.12); ¹H NMR (400 MHz, CDCl₃) δ 10.21 (s, 1H), 9.91 (d, $J = 10.8$ Hz, 2H), 8.94 (s, 1H), 8.18 (d, $J = 10.8$ Hz, 2H), 4.45 (q, $J = 7.1$ Hz, 4H), 1.48 (t, $J = 7.1$ Hz, 6H); ¹³C NMR (100 MHz, CDCl₃) δ 193.2, 164.4, 146.7, 144.8, 142.2, 138.1, 130.3, 117.8, 60.4, 14.5. Anal. Calcd for C₁₇H₁₆O₅: C, 67.99; H, 5.37. Found: C, 67.77; H, 5.30.

Di(1-azulenyl)(1,3-diethoxycarbonyl-6-azulenyl)methane (9a). A solution of **8a** (515 mg, 4.02 mmol) and **7** (601

mg, 2.00 mmol) in acetic acid (21 mL) was stirred at room temperature for 2.5 d under an Ar atmosphere. The solvent was removed under reduced pressure. The residue was neutralized with saturated NaHCO₃ and extracted with CH₂Cl₂. The organic layer was washed with water, dried with MgSO₄, and concentrated under reduced pressure. Purification of the residue by column chromatography on silica gel with CH₂Cl₂ afforded **9a** (301 mg, 28%) as blue crystals, a diastereomeric mixture of 1,3-bis{(1-azulenyl)[1,3-bis(ethoxycarbonyl)-6-azulenyl]methyl}azulene (**10a**) (181 mg, 19%) as deep brown powder, and the recovered **8a** (133 mg, 26%).

9a: mp 158.1–159.2 °C (ethyl acetate/hexane); MS (70 eV) *m/z* (rel intensity) 538 (M⁺, 87%), 267 (M⁺ – C₁₆H₁₅O₄, 100); IR (KBr disk) ν_{\max} 1688 (s, C=O) cm⁻¹; UV-vis (CH₂Cl₂) λ_{\max} , nm (log ϵ) 236 (4.79), 275 (4.88), 294 (4.92), 312 (4.82), 336 sh (4.35), 343 sh (4.32), 367 (4.36), 381 sh (4.33), 495 sh (3.08), 529 sh (3.03), 588 sh (2.91), 646 sh (2.76), 717 sh (2.29); ¹H NMR (400 MHz, CDCl₃) δ 9.62 (d, *J* = 11.0 Hz, 2H), 8.77 (s, 1H), 8.32 (d, *J* = 9.8 Hz, 2H), 8.24 (d, *J* = 9.8 Hz, 2H), 7.75 (d, *J* = 11.0 Hz, 2H), 7.55 (dd, *J* = 10.0, 9.8 Hz, 2H), 7.41 (d, *J* = 3.8 Hz, 2H), 7.30 (d, *J* = 3.8 Hz, 2H), 7.14 (dd, *J* = 10.0, 9.8 Hz, 2H), 7.03 (s, 1H), 7.02 (dd, *J* = 9.8, 9.8 Hz, 2H), 4.38 (q, *J* = 7.1 Hz, 4H), 1.40 (t, *J* = 7.1 Hz, 6H); ¹³C NMR (100 MHz, CDCl₃) δ 165.0, 160.3, 142.8, 142.7, 141.2, 138.4 (2C), 137.8, 137.2, 135.2, 133.7, 132.0, 131.3, 123.2, 122.5, 117.0, 116.2, 59.9, 48.0, 14.5. Anal. Calcd for C₃₇H₃₀O₄: C, 82.50; H, 5.61. Found: C, 82.29; H, 5.84.

10a: major (**A**):minor (**B**) = 58:42; mp 216.0–217.0 °C (ethyl acetate/hexane); MS (FAB) *m/z* 948 (M⁺); IR (KBr disk) ν_{\max} 1690 (s, C=O) cm⁻¹; UV-vis (CH₂Cl₂) λ_{\max} , nm (log ϵ) 236 (5.01), 277 (5.08), 296 (5.11), 303 (5.11), 311 sh (5.10), 336 sh (4.59), 368 (4.61), 380 sh (4.60), 424 sh (3.82), 495 sh (3.39), 530 sh (3.27), 592 sh (3.09), 651 sh (2.94), 716 sh (2.51); ¹H NMR (600 MHz, CDCl₃) for **A**, δ 9.51 (d, *J* = 11.1 Hz, 4H), 8.73 (s, 2H), 8.28 (d, *J* = 9.5 Hz, 2H), 8.24 (d, *J* = 9.7 Hz, 2H), 8.12 (d, *J* = 9.7 Hz, 2H), 7.64 (d, *J* = 11.1 Hz, 4H), 7.54 (t and dd, *J* = 10.1 Hz and *J* = 9.9, 9.9 Hz, 3H), 7.25 or 7.24 (d, *J* = 3.8 Hz, 2H), 7.20 (d, *J* = 3.8 Hz, 2H), 7.14 (dd, *J* = 9.9, 9.5 Hz, 2H), 7.04 (s, 1H), 7.01 (dd, *J* = 10.1, 9.7 Hz, 2H), 6.97 (dd, *J* = 9.9, 9.7 Hz, 2H), 6.96 (s, 2H), 4.38 (q, *J* = 7.1 Hz, 8H), 1.40 (t, *J* = 7.1 Hz, 12H); ¹H NMR (600 MHz, CDCl₃) for **B**, δ 9.50 (d, *J* = 11.0 Hz, 4H), 8.76 (s, 2H), 8.27 (d, *J* = 9.7 Hz, 2H), 8.23 (d, *J* = 9.2 Hz, 2H), 8.02 (d, *J* = 9.7 Hz, 2H), 7.62 (d, *J* = 11.0 Hz, 4H), 7.52 (t, *J* = 10.1 Hz, 1H), 7.46 (dd, *J* = 9.9, 9.7 Hz, 2H), 7.25 or 7.24 (d, *J* = 3.8 Hz, 2H), 7.20 (d, *J* = 3.8 Hz, 2H), 7.05 (dd, *J* = 9.7, 9.2 Hz, 2H), 7.04 (dd, *J* = 10.1, 9.7 Hz, 2H), 6.93 (s, 2H), 6.91 (dd, *J* = 9.9, 9.7 Hz, 2H), 6.87 (s, 1H), 4.40 (q, *J* = 7.1 Hz, 8H), 1.43 (t, *J* = 7.1 Hz, 12H); ¹³C NMR (150 MHz, CDCl₃) δ 165.0 (2C), 159.9, 159.7, 142.9, 142.8, 142.7, 142.6, 141.2, 141.1, 140.3, 139.8, 138.4, 138.3 (2C or 3C), 138.2 (2C or 1C), 138.1, 137.8 (2C), 137.3, 137.2, 136.3, 136.2, 135.1 (2C), 134.4, 134.2, 133.8, 133.7, 131.9 (2C), 130.8, 130.6, 130.4, 130.3, 123.2 (2C), 123.1 (2C), 122.5, 122.3, 116.9, 116.8, 116.2 (2C), 59.9 (2C), 48.0 (2C), 14.6, 14.5. Anal. Calcd for C₆₄H₅₂O₈: C, 80.99; H, 5.52. Found: C, 80.72; H, 5.80.

Bis(3,6-di-tert-butyl-1-azulenyl)(1,3-diethoxycarbonyl-6-azulenyl)methane (9b). The same procedure as was used for the preparation of **9a** was adopted. The reaction of **8b** (291 mg, 1.21 mmol) with **7** (181 mg, 0.603 mmol) in acetic acid (6 mL) at room temperature for 3.5 d followed by chromatographic purification on silica gel with CH₂Cl₂ afforded **9b** (369 mg, 80%) as dark green powder. Mp 288.0–294.0 °C dec (ethyl acetate/hexane); MS (FAB) *m/z* 762 (M⁺); IR (KBr disk) ν_{\max} 1694 (s, C=O) cm⁻¹; UV-vis (CH₂Cl₂) λ_{\max} , nm (log ϵ) 236 (4.72), 279 (4.87), 304 (5.02), 339 sh (4.38), 375 (4.34), 435 sh (3.61), 523 sh (3.20), 602 sh (2.85), 663 sh (2.72), 734 sh (2.22); ¹H NMR (400 MHz, CDCl₃) δ 9.60 (d, *J* = 11.0 Hz, 2H), 8.74 (s, 1H), 8.60 (d, *J* = 10.6 Hz, 2H), 8.15 (d, *J* = 10.6 Hz, 2H), 7.73 (d, *J* = 11.0 Hz, 2H), 7.35 (s, 2H), 7.23 (dd, *J* = 10.6, 2.0 Hz, 2H), 7.10 (dd, *J* = 10.6, 2.0 Hz, 2H), 6.93 (s, 1H), 4.38 (q, *J* = 7.1 Hz, 4H), 1.50 (s, 18H), 1.41 (t, *J* = 7.1 Hz, 6H), 1.40 (s, 18H); ¹³C NMR (100 MHz, CDCl₃) δ 165.2, 161.3, 161.0,

142.7, 142.5, 138.4, 138.1, 136.2, 135.0, 134.8, 134.4, 132.2 (2C), 128.6, 119.8, 119.0, 115.9, 59.2, 47.3, 38.3, 33.2, 32.2, 31.8, 14.6. Anal. Calcd for C₅₃H₆₂O₄: C, 83.42; H, 8.19. Found: C, 83.18; H, 8.43.

(1,3-Diethoxycarbonyl-6-azulenyl)bis(6-methoxy-1-azulenyl)methane (9c). A Teflon vessel (9.1 mL) was filled with **8c** (634 mg, 4.01 mmol), **7** (601 mg, 2.00 mmol), and a solution of 50% acetic acid/CH₂Cl₂. The mixture was left at 10 kbar for 24 h (40 °C). The reaction mixture was worked up and concentrated under reduced pressure. Purification of the residue by column chromatography on silica gel with CH₂Cl₂ and GPC with CHCl₃ afforded **9c** (307 mg, 26%) as deep red crystals, a diastereomeric mixture of 1,3-bis{[1,3-bis(ethoxycarbonyl)-6-azulenyl]([6-methoxy-1-azulenyl)methyl]-6-methoxyazulene (**10b**) (189 mg, 18%) as reddish brown powder, and the recovered **8c** (101 mg, 16%). The reaction of **8c** (158 mg, 1.00 mmol) with **7** (149 mg, 0.496 mmol) in acetic acid (5 mL) at room temperature for 7 h followed by chromatographic purification on silica gel with CH₂Cl₂ and GPC with CHCl₃ afforded **9c** (67 mg, 23%), **10b** (25 mg, 10%), and the recovered **8c** (52 mg, 33%).

9c: mp 173.5–174.4 °C (ethyl acetate/hexane); MS (70 eV) *m/z* (rel intensity) 598 (M⁺, 86%), 442 (M⁺ – C₁₁H₁₀O⁺ + H, 100), 327 (M⁺ – C₁₆H₁₅O₄, 90), 158 (C₁₁H₁₀O⁺, 50); IR (KBr disk) ν_{\max} 1688 (s, C=O) cm⁻¹; UV-vis (CH₂Cl₂) λ_{\max} , nm (log ϵ) 234 (4.69), 278 sh (4.77), 310 (5.06), 366 (4.47), 380 sh (4.35), 430 sh (3.54), 494 sh (3.22), 532 sh (3.11), 584 sh (2.76); ¹H NMR (400 MHz, CDCl₃) δ 9.61 (d, *J* = 11.3 Hz, 2H), 8.76 (s, 1H), 8.16 (d, *J* = 10.8 Hz, 2H), 8.08 (d, *J* = 10.9 Hz, 2H), 7.77 (d, *J* = 11.3 Hz, 2H), 7.18 (d, *J* = 3.9 Hz, 2H), 7.12 (d, *J* = 3.9 Hz, 2H), 6.89 (s, 1H), 6.75 (dd, *J* = 10.8, 2.7 Hz, 2H), 6.63 (dd, *J* = 10.9, 2.7 Hz, 2H), 4.38 (q, *J* = 7.1 Hz, 4H), 3.87 (s, 6H), 1.41 (t, *J* = 7.1 Hz, 6H); ¹³C NMR (100 MHz, CDCl₃) δ 167.4, 165.1, 160.7, 142.7 (2C), 138.4, 136.7, 136.5, 134.0, 133.1, 132.6, 132.2, 131.1, 117.9, 116.0, 110.2, 109.5, 59.9, 55.8, 48.0, 14.6. Anal. Calcd for C₃₉H₃₄O₆: C, 78.24; H, 5.72. Found: C, 78.18; H, 5.90.

10b: major (**A**):minor (**B**) = 58:42; mp 159.2–161.0 °C (ethyl acetate/hexane); MS (FAB) *m/z* 1038 (M⁺); IR (KBr disk) ν_{\max} 1690 (s, C=O) cm⁻¹; UV-vis (CH₂Cl₂) λ_{\max} , nm (log ϵ) 234 (4.96), 277 (4.96), 311 (5.26), 367 (4.71), 381 sh (4.64), 440 sh (3.81), 491 sh (3.57), 529 sh (3.39), 584 sh (3.02); ¹H NMR (600 MHz, acetone-*d*₆) for **A**, δ 9.47 (d, *J* = 10.0 Hz, 4H), 8.55 (s, 2H), 8.31 (d, *J* = 11.1 Hz, 2H), 8.23 (d, *J* = 10.9 Hz, 2H), 8.14 (d, *J* = 10.7 Hz, 2H), 7.82 (d, *J* = 10.0 Hz, 4H), 7.10 (d, *J* = 3.9 Hz, 2H), 7.07 (s, 2H), 7.07 (d, *J* = 3.9 Hz, 2H), 6.97 (s, 1H), 6.78 (dd, *J* = 10.7, 2.3 Hz, 2H), 6.71 (d, *J* = 11.1 Hz, 2H), 6.69 (dd, *J* = 10.9, 2.3 Hz, 2H), 4.31 (q, *J* = 7.1 Hz, 8H), 3.89 (s, 6H), 3.83 (s, 3H), 1.35 (t, *J* = 7.1 Hz, 12H); ¹H NMR (600 MHz, acetone-*d*₆) for **B**, δ 9.53 (d, *J* = 11.0 Hz, 4H), 8.61 (s, 2H), 8.34 (d, *J* = 11.1 Hz, 2H), 8.18 (d, *J* = 10.9 Hz, 2H), 8.10 (d, *J* = 10.7 Hz, 2H), 7.85 (d, *J* = 11.0 Hz, 4H), 7.07 (s, 2H), 7.06 (d, *J* = 4.1 Hz, 2H), 7.05 (d, *J* = 4.1 Hz, 2H), 6.94 (s, 1H), 6.73 (dd, *J* = 10.7, 2.5 Hz, 2H), 6.72 (d, *J* = 11.1 Hz, 2H), 6.65 (dd, *J* = 10.9, 2.5 Hz, 2H), 4.34 (q, *J* = 7.1 Hz, 8H), 3.87 (s, 6H), 3.83 (s, 3H), 1.36 (t, *J* = 7.1 Hz, 12H); ¹³C NMR (150 MHz, acetone-*d*₆) δ 168.9 (2C), 168.5 (2C), 165.0, 164.9, 162.4, 162.3, 143.1 (2C), 142.6 (2C), 139.1, 139.0, 137.6, 137.5, 137.4, 137.3, 136.1, 136.0, 134.9, 134.8, 134.5, 134.3 (2C), 134.1, 133.3, 133.2, 133.0 (2C), 132.8 (4C), 131.9 (2C), 118.7, 118.6, 116.8, 116.7, 111.2, 110.9, 110.7, 110.6, 110.4, 110.0, 60.4, 60.3, 56.4, 56.3, 48.4 (2C), 14.8 (2C). Anal. Calcd for C₆₇H₅₈O₁₁: C, 77.44; H, 5.63. Found: C, 77.15; H, 5.88.

Di(1-azulenyl)(1,3-diethoxycarbonyl-6-azulenyl)methylum Hexafluorophosphate (3a·PF₆⁻). DDQ (54 mg, 0.238 mmol) was added at room temperature to a solution of **9a** (105 mg, 0.195 mmol) in CH₂Cl₂ (5 mL). After the solution was stirred at room temperature for 10 min, 60% aqueous HPF₆ (2 mL) and water (20 mL) were added to the reaction mixture. The resulting suspension was filtered with suction. The organic layer was separated, washed with water, dried with MgSO₄, and concentrated under reduced pressure. The residue was

dissolved in a small amount of CH_2Cl_2 and then poured into ether. The precipitated crystals were collected by filtration, washed with ether, and dried in vacuo to give **3a**· PF_6^- (93 mg, 70%) as a green powder. Mp 150.2–152.0 °C dec; MS (FAB) m/z 682 (M^+), 537 ($\text{M}^+ - \text{PF}_6^-$); IR (KBr disk) ν_{max} 1690 (s, C=O), 841 (s, PF_6^-), 558 (m, PF_6^-) cm^{-1} ; UV-vis (MeCN) λ_{max} , nm (log ϵ) 237 (4.66), 254 (4.66), 293 (4.54), 310 (4.55), 361 (4.53), 376 sh (4.66), 422 sh (4.10), 467 sh (3.87), 675 (4.42); ^1H NMR (600 MHz, CDCl_3) δ 9.82 (d, $J = 10.5$ Hz, 2H), 9.05 (s, 1H), 8.83 (d, $J = 9.6$ Hz, 2H), 8.19 (dd, $J = 9.7, 9.7$ Hz, 2H), 8.11 (dd, $J = 9.7, 9.6$ Hz, 2H), 8.06 (d, $J = 9.7$ Hz, 2H), 7.77 (d, $J = 4.5$ Hz, 2H), 7.75 (d, $J = 10.5$ Hz, 2H), 7.74 (d, $J = 4.5$ Hz, 2H), 7.66 (dd, $J = 9.7, 9.7$ Hz, 2H), 4.46 (q, $J = 7.1$ Hz, 4H), 1.47 (t, $J = 7.1$ Hz, 6H); ^{13}C NMR (150 MHz, CDCl_3) δ 164.5 (2C), 154.8, 153.1, 148.1, 146.7, 146.1, 144.4, 143.9, 141.9, 140.3, 137.2, 136.9, 136.3, 134.6, 134.4, 127.9, 118.3, 60.6, 14.5. Anal. Calcd for $\text{C}_{37}\text{H}_{29}\text{O}_4\text{PF}_6$: C, 65.11; H, 4.28. Found: C, 64.90; H, 4.38.

Bis(3,6-di-tert-butyl-1-azulenyl)(1,3-diethoxycarbonyl-6-azulenyl)methylium Hexafluorophosphate (3b· PF_6^-). The same procedure as was used for the preparation of **3a**· PF_6^- was adopted. The reaction of **9b** (380 mg, 0.498 mmol) with DDQ (136 mg, 0.599 mmol) in CH_2Cl_2 (50 mL) at room temperature for 10 min followed by the treatment with 60% aqueous HPF_6 (5 mL) and water (50 mL) afforded **3b**· PF_6^- (361 mg, 80%) as a deep green powder. Mp >300 °C; MS (FAB) m/z 761 ($\text{M}^+ - \text{PF}_6^-$); IR (KBr disk) ν_{max} 1694 (s, C=O), 841 (s, PF_6^-), 558 (m, PF_6^-) cm^{-1} ; UV-vis (MeCN) λ_{max} , nm (log ϵ) 226 sh (4.72), 254 (4.80), 330 (4.63), 364 (4.69), 447 sh (4.10), 497 sh (3.87), 720 (4.59); ^1H NMR (600 MHz, CDCl_3) δ 9.84 (d, $J = 10.5$ Hz, 2H), 9.06 (d, $J = 11.0$ Hz, 2H), 9.04 (s, 1H), 8.21 (dd, $J = 11.0, 2.0$ Hz, 2H), 7.90 (br d, $J = 10.1$ Hz, 2H), 7.80 (br d, $J = 10.5$ Hz, 2H), 7.69 (br d, $J = 10.1$ Hz, 2H), 7.36 (br s, 2H), 4.47 (q, $J = 7.1$ Hz, 4H), 1.54 (s, 18H), 1.48 (t, $J = 7.1$ Hz, 6H), 1.44 (s, 18H); ^{13}C NMR (150 MHz, CDCl_3) δ 169.8, 164.7, 159.9, 153.7, 150.0, 148.6 (2C), 146.1, 143.9, 141.9, 139.6, 138.9, 137.3, 134.5, 133.5 (2C), 132.6, 118.0, 60.5, 39.5, 33.4, 31.5, 31.0, 14.5. Anal. Calcd for $\text{C}_{53}\text{H}_{61}\text{O}_4\text{PF}_6$: C, 70.18; H, 6.78. Found: C, 70.07; H, 6.78.

Bis(6-methoxy-1-azulenyl)(1,3-diethoxycarbonyl-6-azulenyl)methylium Hexafluorophosphate (3c· PF_6^-). The same procedure as was used for the preparation of **3a**· PF_6^- was adopted. The reaction of **9c** (91 mg, 0.15 mmol) with DDQ (42 mg, 0.19 mmol) in CH_2Cl_2 (15 mL) at room temperature for 10 min followed by the treatment with 60% aqueous HPF_6 (1.5 mL) and water (15 mL) afforded **3c**· PF_6^- (99 mg, 88%) as a green powder. Mp 146.5–147.8 °C dec; MS (FAB) m/z 742 (M^+), 597 ($\text{M}^+ - \text{PF}_6^-$); IR (KBr disk) ν_{max} 1690 (s, C=O), 841 (s, PF_6^-), 558 (m, PF_6^-) cm^{-1} ; UV-vis (MeCN) λ_{max} , nm (log ϵ) 225 (4.57), 252 (4.61), 300 (4.46), 348 (4.65), 364 (4.66), 422 sh (4.22), 668 (4.53); ^1H NMR (600 MHz, CDCl_3) δ 9.81 (d, $J = 10.7$ Hz, 2H), 9.03 (s, 1H), 8.59 (d, $J = 11.2$ Hz, 2H), 7.88 (d, $J = 11.2$ Hz, 2H), 7.74 (d, $J = 10.8$ Hz, 2H), 7.61 (dd, $J = 11.2, 2.9$ Hz, 2H), 7.51 (d, $J = 4.6$ Hz, 2H), 7.37 (d, $J = 4.6$ Hz, 2H), 7.16 (dd, $J = 11.2, 2.9$ Hz, 2H), 4.46 (q, $J = 7.1$ Hz, 4H), 4.07 (s, 6H), 1.47 (t, $J = 7.1$ Hz, 6H); ^{13}C NMR (150 MHz, CDCl_3) δ 172.9, 164.6, 163.2, 153.8, 149.5, 146.3, 143.9, 142.4, 141.3, 141.1, 139.8, 137.0, 135.2, 134.8, 127.7, 124.4, 120.7, 118.0, 60.5, 57.6, 14.5. Anal. Calcd for $\text{C}_{39}\text{H}_{33}\text{O}_6\text{PF}_6$: C, 63.08; H, 4.48. Found: C, 62.80; H, 4.67.

Azulene-1,3-diylbis[(1-azulenyl)(1,3-diethoxycarbonyl-6-azulenyl)methylium] Bis(hexafluorophosphate) (4a· 2PF_6^-). The same procedure as was used for the preparation of **3a**· PF_6^- was adopted. The reaction of **10a** (138 mg, 0.145 mmol) with DDQ (81 mg, 0.36 mmol) in CH_2Cl_2 (15 mL) at room temperature for 10 min followed by the treatment with 60% aqueous HPF_6 (2 mL) and water (20 mL) afforded **4a**· 2PF_6^- (140 mg, 78%) as a dark green powder. Mp 215.2–216.5 °C dec; MS (FAB) m/z 1091 ($\text{M}^+ - \text{PF}_6^-$), 946 ($\text{M}^+ - 2\text{PF}_6^-$); IR (KBr disk) ν_{max} 1692 (s, C=O), 843 (s, PF_6^-), 558 (m, PF_6^-) cm^{-1} ; UV-vis (MeCN) λ_{max} , nm (log ϵ) 227 (4.60), 225 (4.61), 301 (4.49), 357 (4.62), 421 sh (4.30), 466 sh (4.23), 603 (4.06),

712 (4.30). Anal. Calcd for $\text{C}_{64}\text{H}_{50}\text{O}_8\text{P}_2\text{F}_{12}$: C, 62.14; H, 4.07. Found: C, 62.15; H, 4.23.

6-Methoxyazulene-1,3-diylbis[(1,3-diethoxycarbonyl-6-azulenyl)(6-methoxy-1-azulenyl)methylium] Bis(hexafluorophosphate) (4b· 2PF_6^-). The same procedure as was used for the preparation of **3a**· PF_6^- was adopted. The reaction of **10b** (187 mg, 0.180 mmol) with DDQ (99 mg, 0.44 mmol) in CH_2Cl_2 (15 mL) at room temperature for 10 min followed by the treatment with 60% aqueous HPF_6 (2 mL) and water (15 mL) afforded **4b**· 2PF_6^- (179 mg, 75%) as a dark green powder. Mp 209.5–211.0 °C dec; MS (FAB) m/z 1181 ($\text{M}^+ - \text{PF}_6^-$), 1036 ($\text{M}^+ - 2\text{PF}_6^-$); IR (KBr disk) ν_{max} 1692 (s, C=O), 841 (s, PF_6^-), 558 (m, PF_6^-) cm^{-1} ; UV-vis (MeCN) λ_{max} , nm (log ϵ) 227 (4.76), 255 (4.77), 301 sh (4.65), 357 (4.78), 421 sh (4.46), 603 (4.21), 712 (4.46). Anal. Calcd for $\text{C}_{67}\text{H}_{56}\text{O}_{11}\text{P}_2\text{F}_{12}$: C, 60.64; H, 4.25. Found: C, 60.90; H, 4.23.

Potassium bis(3,6-di-tert-butyl-1-azulenyl)(1,3-diethoxycarbonyl-6-azulenyl)methylide ($\text{K}^+\cdot\text{3b}^-$): ^1H NMR (600 MHz, tetrahydrofuran- d_8) δ 8.46 (d, $J = 10.4$ Hz, 2H), 8.19 (br d, $J = 10.0$ Hz, 2H), 7.26 (br s, 2H), 7.16 (dd, $J = 10.4, 1.9$ Hz, 2H), 7.13 (s, 1H), 7.12 (br d, $J = 10.0$ Hz, 2H), 7.05 (d, $J = 12.6$ Hz, 2H), 5.89 (d, $J = 12.6$ Hz, 2H), 4.11 (q, $J = 7.1$ Hz, 4H), 1.53 (s, 18H), 1.49 (s, 18H), 1.28 (t, $J = 7.1$ Hz, 6H); ^{13}C NMR (150 MHz, tetrahydrofuran- d_8) δ 169.0, 161.7, 144.5, 139.7, 139.6, 138.7, 137.6, 135.5, 135.4, 132.6, 128.7, 128.2, 126.4, 121.1, 120.2, 119.0, 114.1, 59.5, 40.0, 35.2, 34.0, 33.5, 16.6. A signal is missing.

Reaction of $\text{K}^+\cdot\text{3b}^-$ with Oxygen. To a solution of **9b** (111 mg, 0.145 mmol) in tetrahydrofuran (10 mL) was added *t*-BuOK (555 mg, 4.95 mmol). After the solution was stirred at room temperature for 90 min under an oxygen atmosphere, the reaction mixture was poured into water and extracted with CH_2Cl_2 . The organic layer was dried with MgSO_4 and concentrated under reduced pressure. Purification of the residue by column chromatography on silica gel with CH_2Cl_2 afforded bis-(3,6-di-tert-butyl-1-azulenyl)ketone (**13**) (40 mg, 54%) as purple crystals. The aqueous layer was acidified with 2 N HCl and extracted with CH_2Cl_2 . The organic layer was dried with MgSO_4 and concentrated under reduced pressure. Purification of the residue by GPC with CHCl_3 afforded a mixture of diethyl 5- and 6-formylindene-1,3-dicarboxylate (**15a** and **15b**) (12 mg, 29%).

13: mp 212.8–214.2 °C; MS (70 eV) m/z (rel intensity) 506 (M^+ , 100), 491 ($\text{M}^+ - \text{Me}$, 64), 449 ($\text{M}^+ - t\text{-Bu}$, 56); IR (KBr disk) ν_{max} 1582 (s, C=O) cm^{-1} ; UV-vis (CH_2Cl_2) λ_{max} , nm (log ϵ) 295 (4.64), 329 (4.49), 427 (4.36), 549 (3.04), 594 sh (2.90), 655 sh (2.34); ^1H NMR (400 MHz, CDCl_3) δ 9.50 (d, $J = 10.6$ Hz, 2H), 8.79 (d, $J = 10.9$ Hz, 2H), 8.05 (s, 2H), 7.60 (dd, $J = 10.6, 1.9$ Hz, 2H), 7.55 (dd, $J = 10.9, 1.9$ Hz, 2H), 1.59 (s, 18H), 1.48 (s, 18H); ^{13}C NMR (100 MHz, CDCl_3) δ 188.9, 162.9, 140.8, 139.5, 138.2, 137.8, 137.0, 136.2, 126.4, 125.2, 122.8, 38.5, 33.0, 31.9, 31.8. Anal. Calcd for $\text{C}_{37}\text{H}_{46}\text{O}$: C, 87.69; H, 9.15. Found: C, 87.81; H, 9.15.

15a and 15b: major [**A** (**15b**):minor [**B** (**15a**)] = 64:36; colorless oil; MS (70 eV) m/z (rel intensity) 288 (M^+ , 92%), 216 ($\text{M}^+ - \text{COOEt} + \text{H}$, 100); IR (neat) ν_{max} 1732 (s, C=O), 1717 (s, C=O), 1700 (s, C=O) cm^{-1} ; UV-vis (CH_2Cl_2) λ_{max} , nm (log ϵ) 230 (4.08), 254 (3.96), 290 (3.83), 397 sh (2.74); ^1H NMR (400 MHz, C_6D_6) for **A**, δ 9.73 (s, 1H), 8.24 (d, $J = 7.8$ Hz, 1H), 8.17 (s, 1H), 7.55 (d, $J = 7.8$ Hz, 1H), 7.39 (d, $J = 2.2$ Hz, 1H), 4.08–3.98 (m, 3H), 3.84–3.75 (m, 2H), 1.00–0.95 (m, 3H), 0.84–0.80 (m, 3H); ^1H NMR (400 MHz, C_6D_6) for **B**, δ 9.73 (s, 1H), 8.64 (s, 1H), 7.61 (d, $J = 7.8$ Hz, 1H), 7.57 (d, $J = 7.8$ Hz, 1H), 7.32 (d, $J = 2.2$ Hz, 1H), 4.08–3.98 (m, 3H), 3.84–3.75 (m, 2H), 1.00–0.95 (m, 3H), 0.84–0.80 (m, 3H); ^{13}C NMR (100 MHz, C_6D_6) δ 191.3, 191.1, 167.3 (2C), 163.0, 162.9, 146.7, 146.1, 145.4, 142.8, 141.6, 141.4, 137.2, 137.0, 136.9, 135.5, 131.1, 127.8, 125.2, 124.8, 124.6, 123.5, 61.7, 60.8, 55.1, 54.8, 14.1, 13.9.

Potassium 1,3-ethoxycarbonyl-5-formylindene (14): ^1H NMR (400 MHz, tetrahydrofuran- d_8) δ 9.82 (s, 1H), 8.53 (s, 1H), 8.09 (d, $J = 8.3$ Hz, 1H), 7.96 (s, 1H), 7.36 (d, $J = 8.3$

Hz, 1H), 4.23 (q, $J = 6.8$ Hz, 2H), 4.21 (q, $J = 6.8$ Hz, 2H), 1.32 (t, $J = 6.8$ Hz, 2H), 1.31 (t, $J = 6.8$ Hz, 2H); ^{13}C NMR (100 MHz, tetrahydrofuran- d_6) δ 193.4, 167.6, 167.4, 139.5, 135.1, 134.2, 128.6, 126.7, 120.5, 118.5, 107.1, 106.1, 58.5 (2C), 15.3 (2C).

Spectroelectrogram Measurements. A sample solution was prepared by dissolving $\mathbf{3b}^+\text{PF}_6^-$ in acetonitrile containing Et_4NClO_4 (0.1 M) and was degassed through an Ar stream. Spectroelectrogram measurements of $\mathbf{3b}^+$ were carried out in a quartz cell ($1 \times 10 \times 35$ mm) equipped with a Pt mesh and a wire as working and counter electrodes, respectively, which were separated by a glass filter. Electrical current was monitored by a microampere meter. Spectroelectrograms were measured on a fiber optic spectrometer at 10- or 20-s intervals.

Acknowledgment. The present work was supported by a Grant-in-Aid for Scientific Research (No. 14540486 to S.I. and No. 15310069 to T.I.) from the Ministry of Education, Culture, Sports, Science, and Technology, Japan. T.I. also thanks the Showa Shell Sekiyu Foundation for Promotion of Environmental Research and the Murata Science Foundation for financial support.

Supporting Information Available: CV data for $\mathbf{3b}^+$ and $\mathbf{4b}^{2+}$, optimized structure of $\mathbf{3b}^+$, ^1H NMR spectra of $\mathbf{4a}, \mathbf{b}^{2+}, 2\text{PF}_6^-, \text{K}^+\cdot\mathbf{3b}^-$, a mixture of $\mathbf{15a}, \mathbf{b}$, and $\mathbf{14}$, and UV-vis spectrum of $\mathbf{3b}^-$. This material is available free of charge via the Internet at <http://pubs.acs.org>.

JO035053O